Supplementary Information

Advancement of Atmospheric-Vacuum Interfaces for Mass Spectrometers with a focus on Increasing Gas Throughput for Improving Sensitivity

Satendra Prasad[1*], Eloy R. Wouters[1], Jean-Jacques Dunyach[1]

Thermo Fisher Scientific, San Jose, CA 95134

[*]Corresponding author: satendra.prasad@thermofisher.com

Methods and Materials: Simulation Using Ansys CFX.

Computational Fluid Dynamics modeling was performed using the ANSYS CFX program (Release 15.0, Canonsburg, PA) to solve the Navier-Stokes equations for the velocity vector, pressure, and temperature, of the 3D compressible gas flow on a discrete mesh. The 3D system is computationally very large and requires 70,000 to 100,000 iterations to converge. Two different models were created to study the dependence of the slot shape on gas flows. The models include a chamber at atmospheric pressure (not shown in Figure 3) where the capillary (round bore or slotted) originates. The gas emerges from the capillary into the funnel chamber held at 4 Torr, while the following chamber is held at 0.4 Torr. It is noted that this final chamber is only added to allow for an outflow boundary condition, since at these very low pressures the underlying approximations for the Navier-Stokes equations become less valid. However, these are well established for the pressures encountered in the funnel chamber that is the focus of the modeling efforts of the anisotropic expansion of gas emerging from the capillaries. Because of this focus of the study, and also based on the expected Reynolds numbers of the flow which will be highest (~ 5,000) inside the otherwise smooth capillary where an exact approximation of the flow is not required, no modeling of the turbulent energy term was included. A brief study that includes one of the many semi-empirical formulations of the turbulence programmed in the CFX package did not significantly alter the results that are shown in Figure 3. The density of the tetrahedral mesh elements (1.4 million) was chosen to be high enough (and highest in the center of the system) to capture the strongest gradients in the expansion with sufficient detail. The mass flux flowing through the capillaries (no-slip wall and smooth roughness setting boundary condition) was found to increase by the same factor comparing round bore and slotted bore as seen in the experimental results (Figure 2). The boundary conditions of the slotted openings in between the funnel electrodes allow for gas to flow both into and out of the funnel, since a priori we have no knowledge in regards to the gas flow in these slots.

Table S-1: Two separate assays were used in this study to evaluate various aspects that constitute a sensitive and robust mass spectrometer. High chromatographic flow rate challenge the front end ion optics ability to desolvate ions and handle chemical noise that arise from the high volume liquid chromatography stream. Assays classed as small molecule are best suited for high flow rate and compounds used in this study are listed in Table S-1.

Table S-2: However**,** desolvation at high flow rate is also aided by heat from the Heated Electrospray Ionization (HESI) source. This is absent at nano chromatographic flow rate and ion desolvation is largely dependent on the MS inlet capillary temperature. A separate assay targeting six doubly charged peptides spiked in *E. coli* digest (Table S-2) was used to evaluate desolvation efficiency at nano chromatographic flow rate.

Table S-3: Recently multiple alternatives to front end ion optics have been reported and it was unclear on whether the ion optics developed for TSQ Quantiva was at par in performance to superior performing alternatives. This was answered by comparing the TSQ Quantiva ion optics with an orthogonal injection dual Electrodynamic Ion Funnel that has claimed superior performance in sensitivity and in handling chemical background. Comparative results are shown in Table S-3 for peptides at nano chromatographic flow rate.

Figure S-1: With the large MS inlet used in the TSQ Quantiva the MS draws 4.3 fold more gas stream and chemical noise. The ion optics was modified to reduce the chemical background and the orthogonal dual Electrodynamic Ion Funnel was used as benchmark to compare chemical background. Selected ion chromatograms from LC-MRM analysis using TSQ Quantiva ion optics and orthogonal dual Electrodynamic Ion Funnel are compared for Reserpine (A), Oxycodone (B), Ketoconazole (C), Paroxetine (D), and Buprenorphine (E).

Figure S-2: In the absence of heat from the HESI ion source, such as the case in nano ESI, desolvation largely occurs in the MS inlet capillary. Selected ion chromatograms from LC-MRM analysis using TSQ Quantiva ion optics and orthogonal dual Electrodynamic Ion Funnel are compared for IGSEVYHNLK (F), TFAEALR (G), LVNELTEFAK (H), NVNDVIAPAFVK (I), and HLVDEPQNLIK (J) at 300 nL/min under nano ion source conditions.

Table S-1. List of nine compounds and product ions monitored during SRM analysis.

Compound	$[M+H]^+$	Product Ion (CE)	RT (min)
Oxycodone	316.2	241.1 (27)	1.5
Buprenophine	468.3	414.2 (36) 396.3 (36)	3.0
Paroxetine	330.2	192.1 (19)	4.0
Clonazepam	316.1	270.1 (24)	4.5
Verapamil	455.3	165.1 (25)	4.5
Ketoconazole	531.2	498.1 (29)	3.9
Alprazolam	309.1	281.1 (25)	4.5
Reserpine	609.3	195.1 (38) 174.1 (41)	5.1
Clopidogrel	322.1	212.0 (14)	5.3

Table S-2. List of six parent (2+) and product ions of peptides from BSA and Enolase sample that were monitored during an SRM analysis.

Compound	$[M+xH]^{x+}$	Product Ion (CE)	RT (min)
TFAEALR	404.2 (2+)	488.3 (13) 559.3 (13) 706.4 (13)	11.2
AEFVEVTK	461.7 (2+)	476.3 (15) 575.3 (15) 722.4 (15)	10.9
IGSEVYHNLK	580.3 (2+)	674.4 (22) 773.4 (22) 902.5(22)	9.9
LVNELTEFAK	582.3 (2+)	595.3 (19) 708.4(19) 951.5 (22)	4.5
NVNDVIAPAFVK	643.9 (2+)	745.5 (22) 844.5 (22) 959.6 (22)	16.5
HLVDEPQNLIK	653.4 (2+)	712.4 (22) 956.5 (22) 1055.6 (22)	13.2

Table S-3. A comparative study of sensitivity between Quantiva Ion Optics and orthogonal injection dual Electrodynamic Ion Funnel (o-d-EDIF) using peptides at nano chromatographic flow rate.

	Quantiva Ion Optics		**o-d-EDIF**		
Compound	**Area (% CV)**	**S/N (%CV)**	**Area (% CV)**	**S/N (%CV)**	**Signal Gain (±)**
1.) TFAEALR (100 attomole)	82578 (3.9%)	752 (11.8%)	36118 (7.2%)	405 (10.2%)	+ 2.3 ± 0.24
2.) AEFVEVTK (100 attomole)	363158 (8.1%)	2663 (8.9%)	262585 (3.7%)	1896 (8.8%)	+ 1.4 ± 0.07
3.) IGSEVYHNLK (1 femtomole)	22003 (4.7%)	342 (14.2%)	26763 (2.1%)	291 (2.5%)	- 1.2 ± 0.08
4.) LVNELTEFAK (1 femtomole)	293630 (6.3%)	2757 (9.1%)	197217 (1.0%)	1984 (8.0%)	+ 1.5 ± 8.9
5.) NVNDVIAPAFVK (100 attomole)	15059 (5.1%)	178 (15.2%)	11508 (22.7%)	89 (9.8%)	+ 1.4 ± 0.34
6.) HLVDEPQNLIK (100 attomole)	18517 (6.1%)	325 (12.0%)	15177 (7.7%)	234 (3.7%)	+ 1.2 ± 0.14

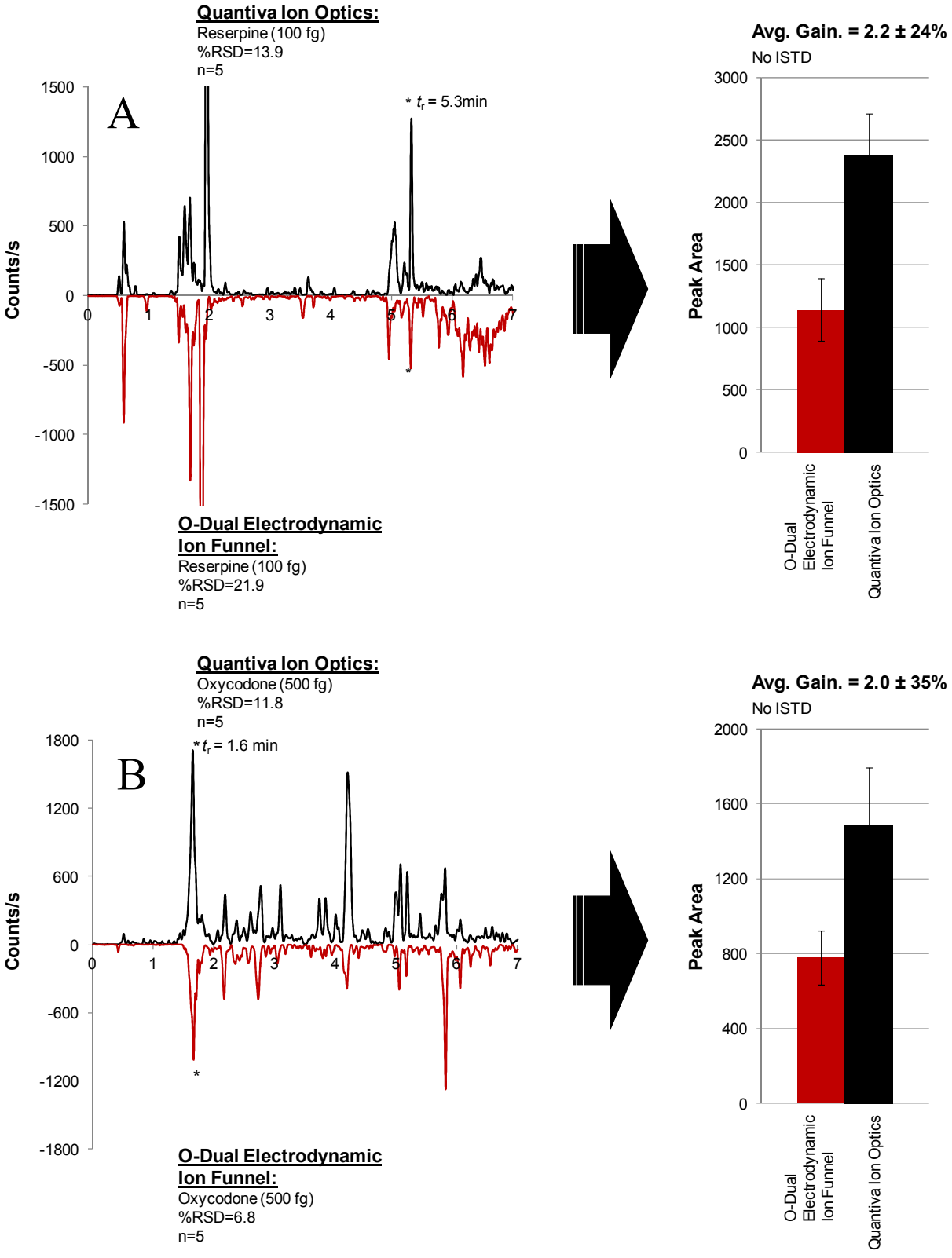
Quantiva Ion Optics:
Reserpine (100 fg)
%RSD=13.9
n=5
A
* t_r = 5.3min
Counts/s
1500
1000
500
0
-500
-1000
-1500
0
1
2
3
4
5
6
7
O-Dual Electrodynamic Ion Funnel:
Reserpine (100 fg)
%RSD=21.9
n=5
Avg. Gain. = 2.2 ± 24%
No ISTD
Peak Area
3000
2500
2000
1500
1000
500
0
O-Dual Electrodynamic Ion Funnel
Quantiva Ion Optics
Quantiva Ion Optics:
Oxycodone (500 fg)
%RSD=11.8
n=5
B
* t_r = 1.6 min
Counts/s
1800
1200
600
0
-600
-1200
-1800
0
1
2
3
4
5
6
7
O-Dual Electrodynamic Ion Funnel:
Oxycodone (500 fg)
%RSD=6.8
n=5
Avg. Gain. = 2.0 ± 35%
No ISTD
Peak Area
2000
1600
1200
800
400
0
O-Dual Electrodynamic Ion Funnel
Quantiva Ion Optics

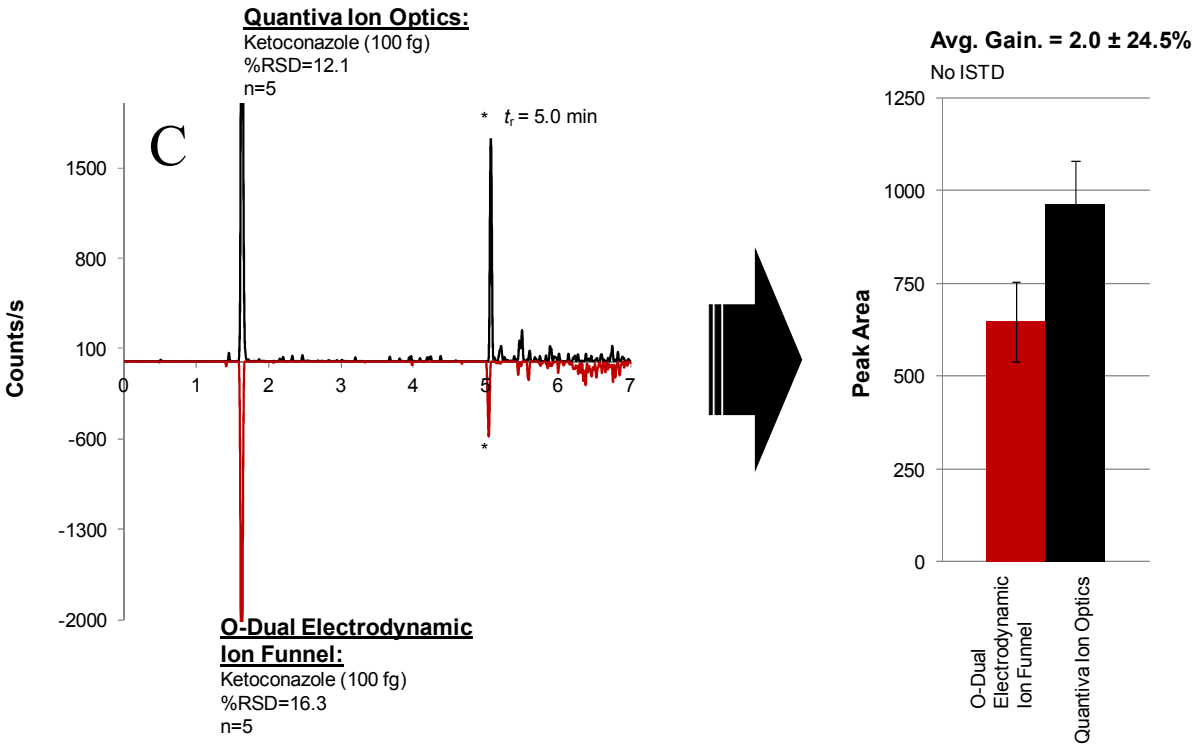
Quantiva Ion Optics:
Ketoconazole (100 fg)
%RSD=12.1
n=5
C
* t_r = 5.0 min
Counts/s
1500
800
100
-600
-1300
-2000
0
1
2
3
4
5
6
7
O-Dual Electrodynamic Ion Funnel:
Ketoconazole (100 fg)
%RSD=16.3
n=5
Avg. Gain. = 2.0 ± 24.5%
No ISTD
Peak Area
1250
1000
750
500
250
0
O-Dual Electrodynamic Ion Funnel
Quantiva Ion Optics

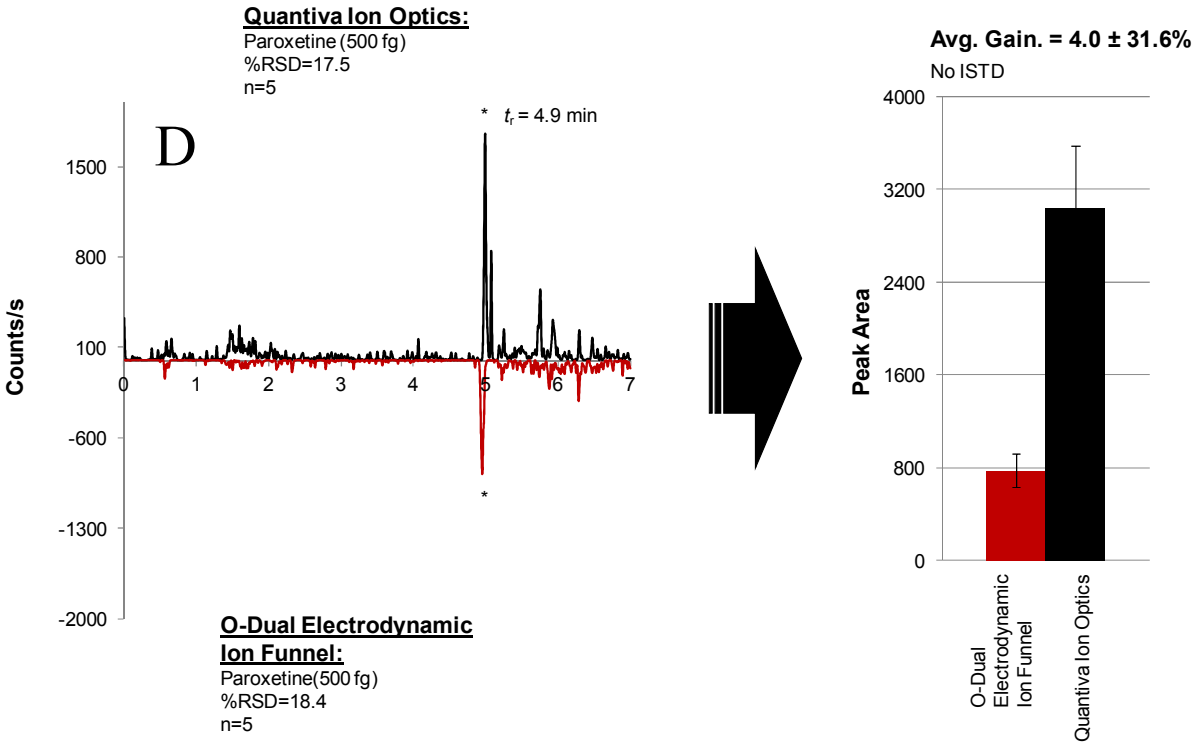
Quantiva Ion Optics:
Paroxetine (500 fg)
%RSD=17.5
n=5
D
* t_r = 4.9 min
Counts/s
1500
800
100
-600
-1300
-2000
0
1
2
3
4
5
6
7
O-Dual Electrodynamic Ion Funnel:
Paroxetine(500 fg)
%RSD=18.4
n=5
Avg. Gain. = 4.0 ± 31.6%
No ISTD
Peak Area
4000
3200
2400
1600
800
0
O-Dual Electrodynamic Ion Funnel
Quantiva Ion Optics

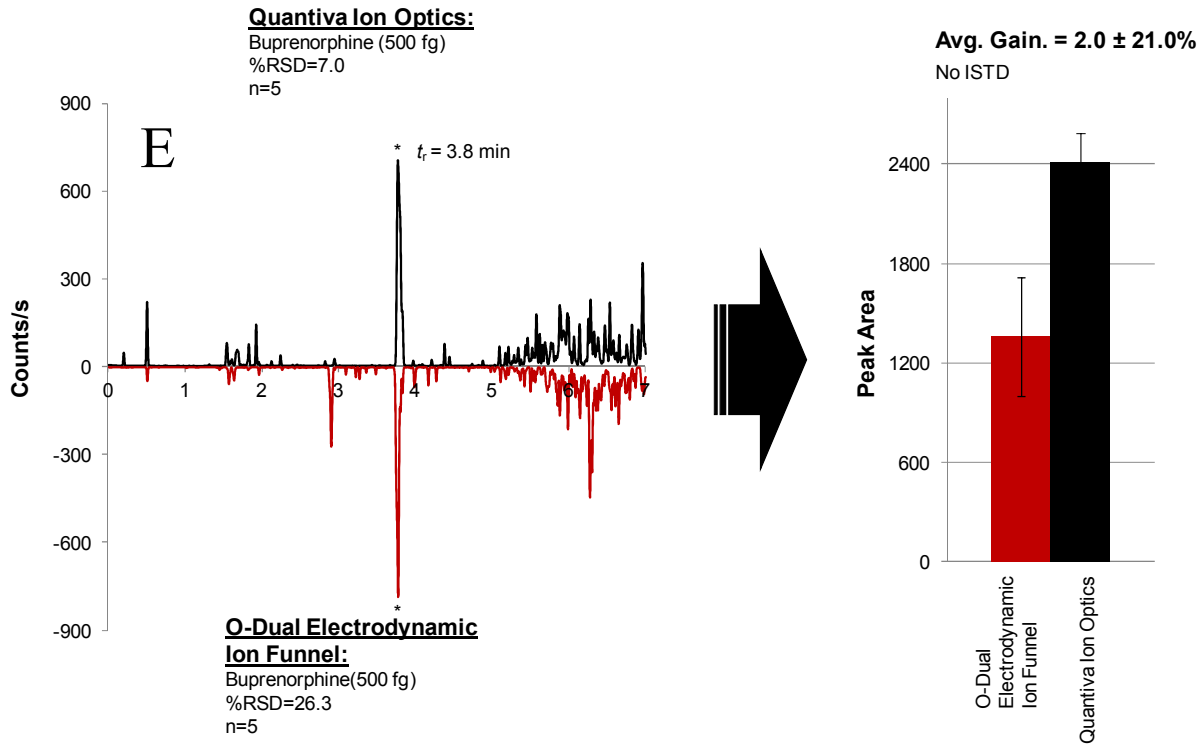

Figure S-1. Shows selected ion chromatograms of Reserpine (A), Oxycodone (B), Ketoconazole (C), Paroxetine (D), and Buprenorphine (E) from LC-MRM analysis done using Quantiva ion optics (black trace) and orthogonal dual Electrodynamic Ion Funnel (red trace). The bar graphs compare peak area from triplicate runs between Quantiva ion optics (black trace) and orthogonal dual Electrodynamic Ion Funnel (red trace)

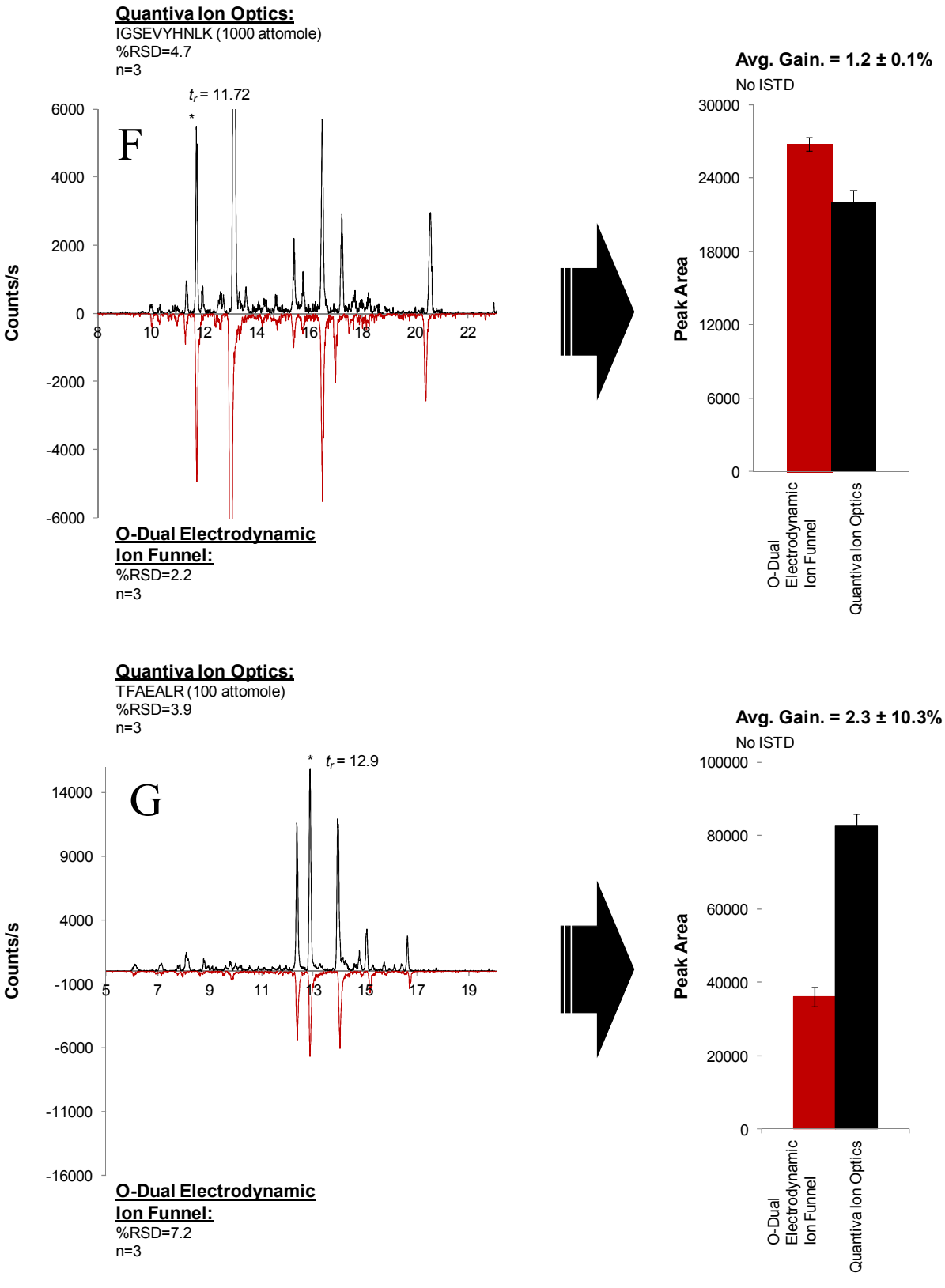
Quantiva Ion Optics:
IGSEVYHNLK (1000 attomole)
%RSD=4.7
n=3
t_r = 11.72
F
Counts/s
O-Dual Electrodynamic Ion Funnel:
%RSD=2.2
n=3
Avg. Gain. = 1.2 ± 0.1%
No ISTD
Peak Area
O-Dual Electrodynamic Ion Funnel
Quantiva Ion Optics
Quantiva Ion Optics:
TFAEALR (100 attomole)
%RSD=3.9
n=3
t_r = 12.9
G
Counts/s
O-Dual Electrodynamic Ion Funnel:
%RSD=7.2
n=3
Avg. Gain. = 2.3 ± 10.3%
No ISTD
Peak Area
O-Dual Electrodynamic Ion Funnel
Quantiva Ion Optics

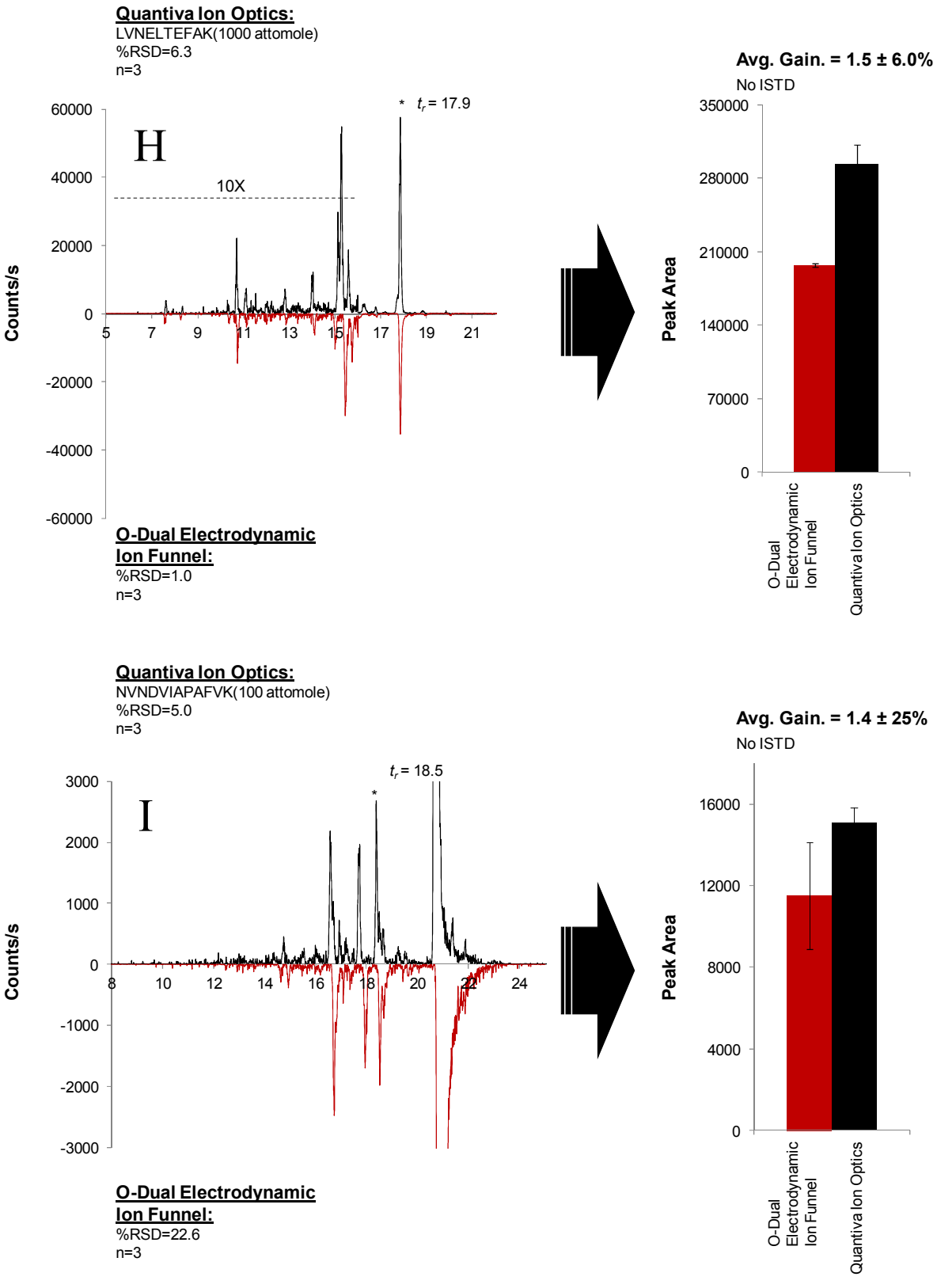
Quantiva Ion Optics:
LVNELTEFAK(1000 attomole)
%RSD=6.3
n=3
H
10X
* t_r = 17.9
Counts/s
60000
40000
20000
0
-20000
-40000
-60000
5
7
9
11
13
15
17
19
21
O-Dual Electrodynamic Ion Funnel:
%RSD=1.0
n=3
Avg. Gain. = 1.5 ± 6.0%
No ISTD
Peak Area
350000
280000
210000
140000
70000
0
O-Dual Electrodynamic Ion Funnel
Quantiva Ion Optics
Quantiva Ion Optics:
NVNDVIAPAFVK(100 attomole)
%RSD=5.0
n=3
I
t_r = 18.5
*
Counts/s
3000
2000
1000
0
-1000
-2000
-3000
8
10
12
14
16
18
20
22
24
O-Dual Electrodynamic Ion Funnel:
%RSD=22.6
n=3
Avg. Gain. = 1.4 ± 25%
No ISTD
Peak Area
16000
12000
8000
4000
0
O-Dual Electrodynamic Ion Funnel
Quantiva Ion Optics

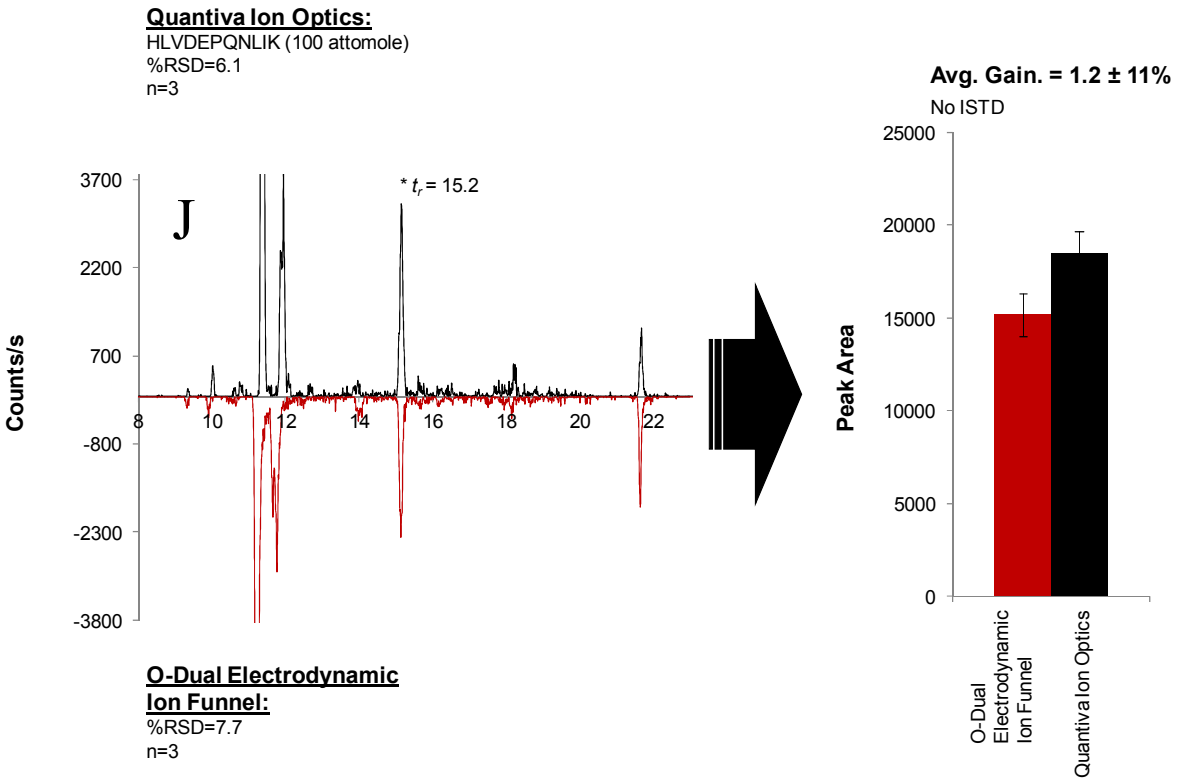

Figure S-2. Shows selected ion chromatograms of IGSEVYHNLK (F), TFAEALR (G), LVNELTEFAK (H), NVNDVIAPAFVK (I), and HLVDEPQNLIK (J) from LC-MRM analysis done using Quantiva ion optics (black trace) and orthogonal dual Electrodynamic Ion Funnel (red trace). The bar graphs compare peak area from triplicate runs between Quantiva ion optics (black trace) and orthogonal dual Electrodynamic Ion Funnel (red trace).